Research of the stress distribution in ceramic composite with bone tissue inclusions

V A Mikushina[1,2] and I Yu Smolin[1,2]

[1]National Research Tomsk State University, 634050 Tomsk, Russia
[2]Institute of Strength Physics and Materials Science SB RAS, 634055 Tomsk, Russia
E-mail: mikushina_93@mail.ru

Abstract. Numerical investigation of features of statistical stress distribution and stress state heterogeneities of the composite "zirconia-based ceramics—cortical bone tissue" is presented in this paper. The finite-difference method is used for modeling the mechanical behavior of composite. Deformation and fracture processes are described using the constitutive model of the elastic-brittle material with damage accumulation and degradation of elastic moduli. Additionally, a fracture criterion based on limiting value of negative pressure in tension regions is used. The effective characteristics (mechanical properties) of the composite were determined on the basis of the data on the mechanical properties of its constituents. Values of effective stress and strain corresponding to the macroscopic fracture: σ = 155 MPa and ε = 0.56 % were found. The evolution of statistical stress distribution in the components of the composite was studied. It was shown that damage accumulation significantly affects the form of stress distribution at the final stages of deformation. Both ceramic matrix and bone tissue inclusions were found to be fractured, bone tissue being fractured under tensile pressure predominantly.

1. Introduction

At present, a primary medical consideration is the treatment of bone defects resulting from mechanical injuries, congenital anomalies or surgical interventions: in dentistry, traumatology, orthopedics, maxillofacial surgery, neurosurgery, and so on. Medical products or tissue engineering constructions based on ceramics are used for repairing large bone defects.

Ceramics for such medical applications are of several types. One of the most popular and effective materials for the manufacturing of implants subjected to active loading is zirconia-based ceramics [1-3]. Zirconia-based ceramic materials are characterized by high strength, as well as high biocompatibility with living tissues of the human body. In order to use ceramics in medicine, it is necessary to have porosity in these materials. First, the porosity makes it possible to decrease the high elastic modulus of ceramics closer to one of the bones. Second, the presence of porosity in the implant allows living bone tissue to fill the pores. As a result, a ceramic matrix composite with bone tissue inclusions is formed. The experimental study of the mechanical properties of such composites is a complex, expensive, and long-term process. In contrast to experimental study, numerical simulation is much less resource-consuming and can be repeatable in different variations. Thus, the development of numerical methods and approaches for the study of mechanical behavior of this composite is a relevant problem.

Computer modeling is widely used to investigate fracture processes and deformation of such materials with heterogeneous structures, the validity of which depends on the quality of the constitutive and computer models adopted. Various approaches and numerical methods are used for evaluating the mechanical properties of composite materials [4–7]. Presently, one of the most promising and extensively developed approaches is a multiscale approach [8–10]. This approach considers various structural features and their effect on the effective mechanical properties of composites. Also probabilistic analysis has attracted particular interest in investigation of heterogeneous materials [11, 12].

The purpose of this paper is a numerical investigation of features of statistical stress distribution and stress state heterogeneities of the composite "zirconia - based ceramics—cortical bone tissue". Numerical investigation of the mechanical behavior of the composite was performed using an elastic-brittle material model and on the base of the finite-difference method.

2. Model description and its numerical implementation

To attain this end, the model structure of the composite "zirconia-based ceramics—cortical bone tissue" was numerically studied in the two-dimensional statement in the uniaxial compression. The model structure of the composite is shown in Figure 1. The structure was specified with explicit consideration for pores. It is suggested that the pores are filled with bone tissue. The percent composition of cortical bone tissue is 13 %. The mechanical and physical properties of the composite components are given in Table 1. For the matrix, we take physical and mechanical characteristics corresponding to the porous zirconia-based ceramics. For the inclusions, we take physical and mechanical characteristics corresponding to cortical bone tissue.

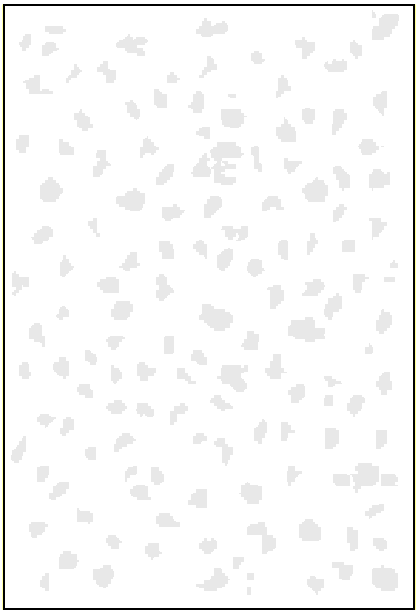

Figure 1. Model structure of the composite used for the simulation.

Table 1. Mechanical and physical properties of the composite components.

Material	Density ρ, g/cm^3	Cohesion *Y*, MPa	Bulk modulus *G*, GPa	Shear modulus *K*, GPa	Coefficient of internal friction α
Porous zirconia	4	80	10	31.2	0.13
Cortical bone	1.85	40	6.15	13.3	0.13

The finite-difference method is used for numerical investigation of deformation and fracture processes in the studied structure of composite. The differential equations of solid mechanics within the Lagrangian description of a continuum are numerically solved. A constitutive model of the elastic-brittle material with damage accumulation and degradation of elastic characteristics is adopted.

The complete system of continuum mechanics equations includes the fundamental conservation laws of mass and momentum (1), geometrical relations (2), and constitutive equations (3)–(7)

$$\frac{d\rho}{dt} + \rho\, div\bar{\upsilon} = 0 \quad \rho\frac{d\upsilon_i}{dt} = \frac{\partial\sigma_{ij}}{\partial x^j} \tag{1}$$

$$\dot{\varepsilon}_{ij} = \frac{1}{2}\left(\frac{\partial\upsilon_i}{\partial x^j} + \frac{\partial\upsilon_j}{\partial x^i}\right) \tag{2}$$

The elastic response is described by the relations (3)

$$\dot{P} = -K\dot{\varepsilon}_{ii}\ ,\ \dot{s}_{ij} = 2G\left[\dot{\varepsilon}_{ij} - \frac{1}{3}\dot{\varepsilon}_{ii}\delta_{ij}\right] \tag{3}$$

Here ρ is the current value of the material density, υ_i is a component of the velocity vector, σ_{ij} is a component of the stress tensor, ε_{ij} is a component of the strain tensor, P is the pressure, s_{ij} is a component of the deviatoric stress tensor, G and K are the shear modulus and bulk modulus, respectively, δ_{ij} is the Kronecker symbol. Here we use decomposition of stress tensor into the pressure and deviator $\sigma_{ij} = -P + s_{ij}$.

Deformation and fracture are modeled using constitutive model of the damageable elastic-brittle material. In this case, we use the governing equations taking account of damage accumulation that is responsible for the degradation of elastic moduli:

$$D(t) = \begin{cases} \displaystyle\int_{t_0}^{t} \frac{(\sigma - \sigma_c)^2}{\sigma_*^2 t_c} dt, & \text{if } \mu_\sigma \geq 0 \\ \displaystyle\int_{t_0}^{t} \frac{(\sigma - \sigma_t)^2}{\sigma_*^2 t_t} dt, & \text{if } \mu_\sigma \leq 0 \end{cases} \tag{4}$$

$$G = G_0(1 - D)\,, K = K_0(1 - D) \tag{5}$$

Here $D(t)$ is the damage function, μ_σ is the Lode–Nadai coefficient, $\sigma = -\alpha J_1 + \sqrt{J_2}$ is the Drucker–Prager stress, α is the coefficient of internal friction, J_1 is the first invariant of the stress tensor, $J_2 = \frac{1}{2}s_{ij}s_{ij}$ is the second invariant of the deviatoric stress tensor, σ_c and σ_t are stress values after which the material begins to accumulate damages in the regions of compression and tension, respectively, with the constraint $\sigma_t \ll \sigma_c$, t_c, t_t are the characteristic fracture times in compression and tension, respectively, and $\sigma_* = \sigma_{0*}(1.01 + \mu_\sigma)^2$ is the model parameter defining the damage accumulation rate. G_0 and K_0 are the initial shear modulus and bulk modulus, respectively.

In order to describe the fracture process, we utilize two fracture criteria. The first is based on the local damage value D (t) (6):

$$D(t) = 1 \tag{6}$$

The second criterion describes fracture due to the critical value of tensile pressure (7):

$$P < P_{cr} < 0 \tag{7}$$

After meeting a fracture criterion, all components of stress tensor are equated to zero, and then the material ceases to resist tension but not compression.

3. Simulation results and analysis

The macroscopic stress-strain curve in compression is presented in Figure 2. Here averaged stress is plotted versus engineering strain. As shown in Figure 2, a linear correlation between averaged stress and strain values in the initial section of the stress-strain curve is observed. Starting from the strain of 0.530 %, this linear correlation is finished. A short plateau caused by the accumulation of the microdamage in the volume of the composite appears in the graph. Microdamage is accumulated with the growth of strain; for this reason, the macrodamage takes place, which implies to the drop of the stress-strain curve.

Point A on the stress-strain curve corresponds to the averaged stress and strain at which the ceramic composite is fractured. The macrofracture takes place for the chosen parameters of the model at following averaged stresses and strains: $\sigma = 155$ MPa and $\varepsilon = 0.56$ %.

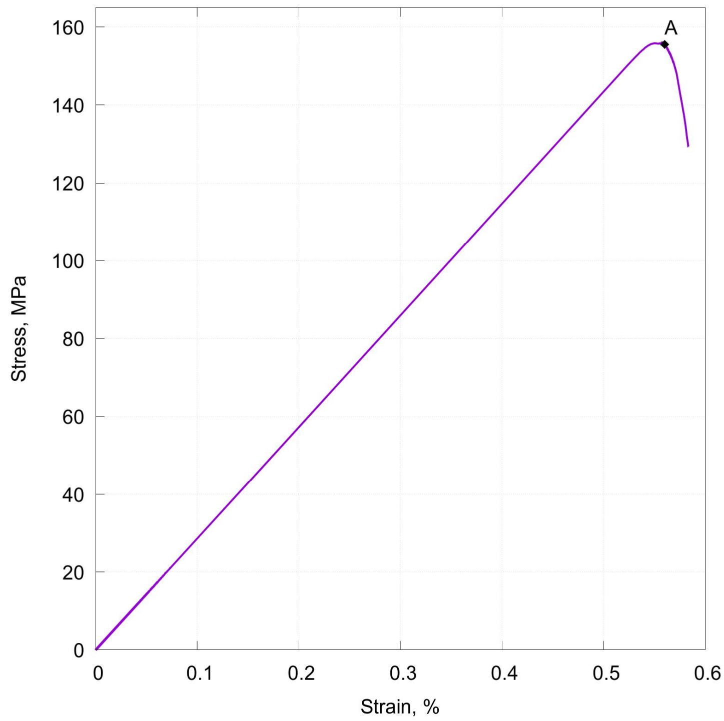

Figure 2. Macroscopic stress-strain curve of the composite "zirconia-based ceramics—cortical bone tissue" in uniaxial compression.

Stress distributions in each of the composite components for studying the features of the evolution of statistical stress distribution were plotted. The distributions of stress tensor horizontal components (along the loading axis) at various stages of deformation are presented in Figure 3. It is notable that at averaged strain values corresponding to the elastic linear section on the stress-strain curve, changes of the statistical distribution form are observed, namely, there is a decrease in distribution peak values and an increase in dispersion. This is due to the fact that a part of the structure of the composite has fractured at mesoscale. This is most clearly seen when strain values correspond to the peak on the stress-strain curve.

At this moment the second peak appears on the statistical distribution in the range of zero stress (fig.3d). This peak is because the damage reaches the critical value and according to the fracture criterion the stresses are nullified. Soon afterwards, the stress-strain curve is coming into the short saturation period with the growth of strains. Thereafter, the drop in the stress-strain curve appears.

Journal of Physics: Conference Series **1459** (2020) 012006 doi:10.1088/1742-6596/1459/1/012006

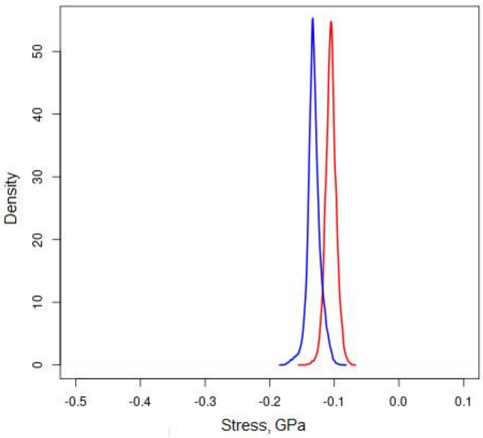

(a) ε = 0.446 %

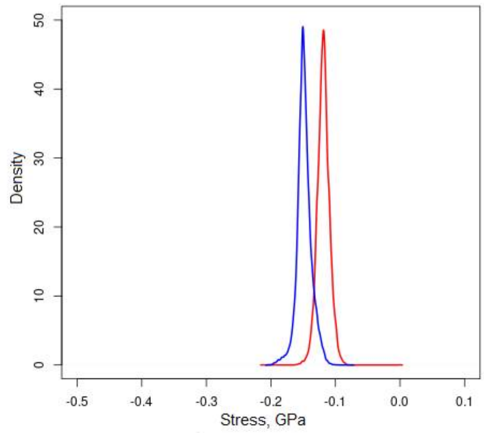

(b) ε = 0.503 %

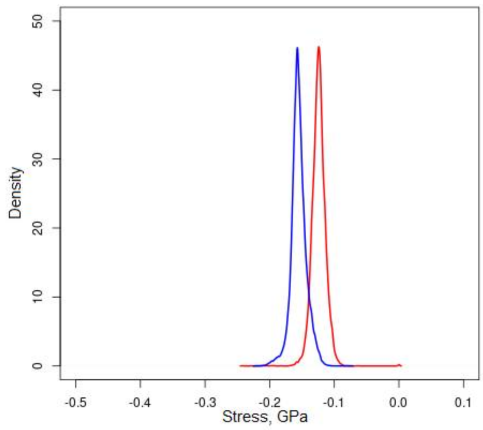

(c) ε = 0.526 %

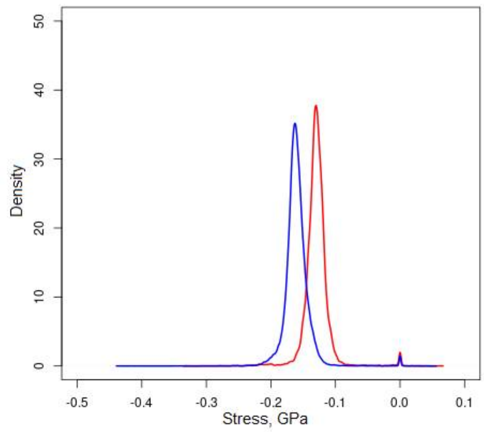

(d) ε = 0.549 %

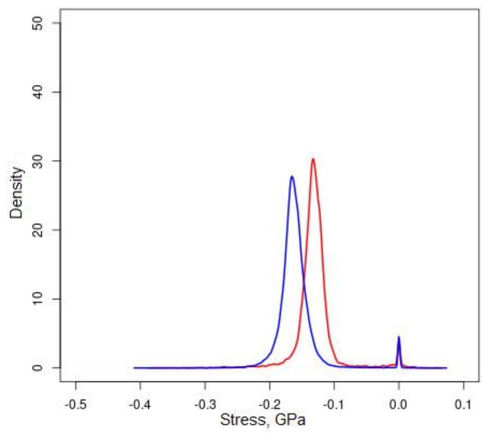

(e) ε = 0.560 %

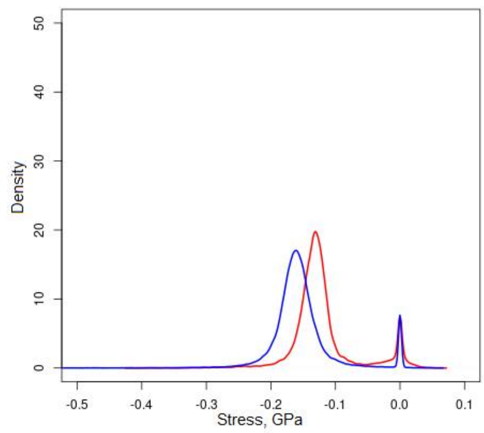

(f) ε = 0.572 %

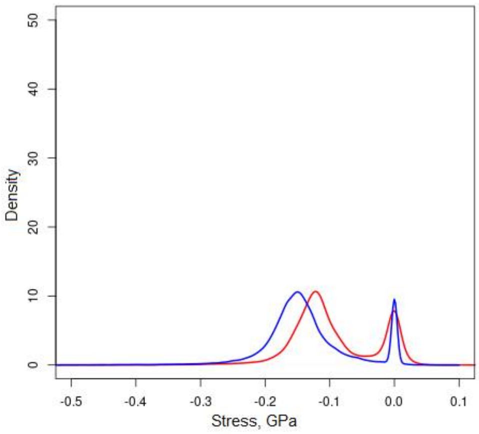

(g) ε = 0.583 %

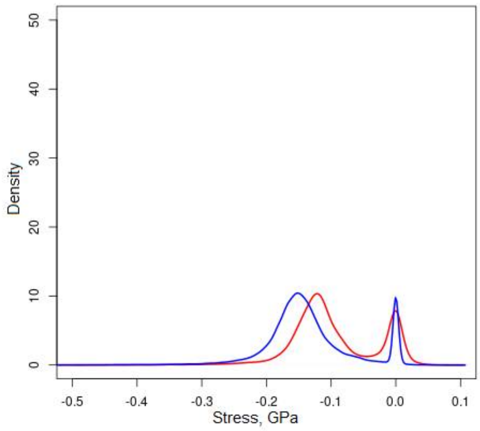

(h) ε = 0.584 %

Figure 3. Statistical stress distribution in the composite components at various strain values: blue color is the distribution in the ceramics; red color is the distribution in the bone tissue.

The fracture patterns of the investigated structure of the composite in compression along the horizontal axis are shown in Fig. 4.

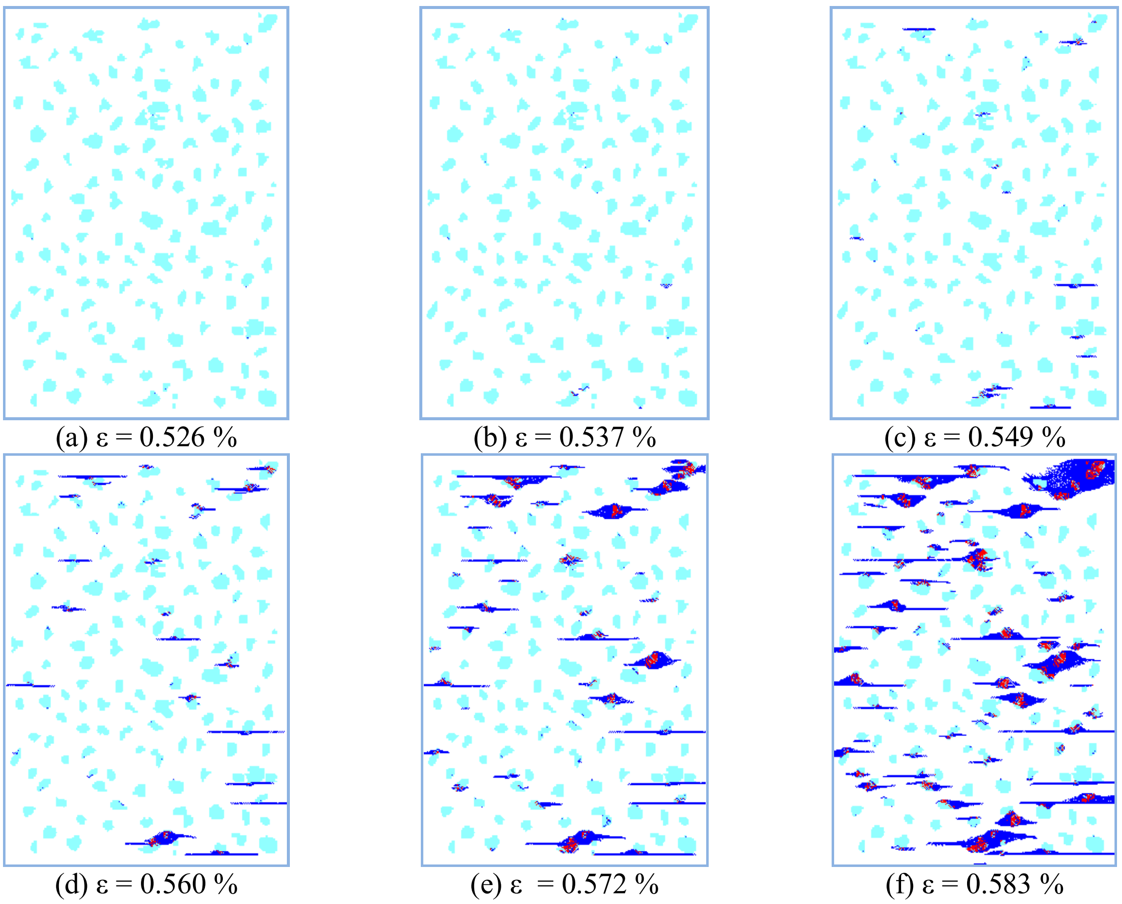

(a) ε = 0.526 % (b) ε = 0.537 % (c) ε = 0.549 %

(d) ε = 0.560 % (e) ε = 0.572 % (f) ε = 0.583 %

Figure 4. Fracture patterns of composite loaded in compression at various strain values.

In Fig. 4 blue color corresponds to the damage fracture criterion, red color corresponds to the tensile pressure fracture criterion. The structure of the composite in an undamaged state at the initial stage of deformation is presented in Figure 4a. When strain value reaches 0.535 %, microdamages nucleate in the material and fracture locations appear on the fracture patterns. Nucleation of the microdamages caused by the structure of the composite occurs in the location of strong stress concentrators. With the growth of strain, the damages are accumulated and propagate in the structure of the composite along the loading axis, forming cracks. This propagation of cracks is typical to the behavior of brittle materials. At strain 0.560 % in the pores filled with bone tissue, the tensile pressure fracture criterion is fulfilled (Fig. 4 d-f). The regions with negative pressure caused by curvilinear interfaces are typical for structurally heterogeneous materials loaded in compression, that is pointed out elsewhere [13, 14].

4. Conclusion

The features of the stress state of the composite ”zirconia-based ceramics—cortical bone tissue“ depending on the properties of its components in uniaxial compression were numerically investigated. The analysis of the macroscopic stress strain curve allowed us to find the limiting values of effective stress and strain corresponding to the macrofracture criterion: σ = 155 MPa and ε = 0.56 %. The effect of damage accumulations on the features of the statistical stress distribution was studied. It is shown that the form of stress distribution changes with increasing of damages. This results in a decrease in the distribution peak values and an increase in the dispersion.

Also, the effect of the heterogeneities of the composite structure on the local fracture of the composite material as well as on the macroscopic stress-strain curve was analyzed. It was shown that the presence of strong stress concentrators in the structure of the composite determines the crack nucleation site and affects crack propagation in the modeled structure. Both ceramic matrix and bone tissue inclusions are found to be fractured, bone tissue being fractured under tensile pressure predominantly.

5. Acknowledgments

The work was carried out within the framework of the Fundamental Research Program of the State Academies of Sciences for 2013–2020, line of research III.23, and with the support of the Tomsk State University Competitiveness Improvement Program.

References

[1] Savchenko N L, Sablina T Y, Sevost'yanova I N, Burlachenko A G, Buyakova S P and Kul'kov S N 2018 *Tech. Phys. Lett.* **44** (8) 663–666
[2] Kulbakin D E, Choinzonov E L, Mukhamedov M R, Buyakov A S, Buyakova S P and Kulkov S N 2019 *IOP Conf. Ser.: Mater. Sci. Eng.* **511** (1) 12006
[3] Kulkov S, Buyakova S, Chatzinikolaidou M and Kocserga I 2015 *J. Silic. Based Compos. Mater.* **4** 155–158
[4] Eremina G M, Smolin A Yu 2019 *Facta Univ. Ser. Mech. Eng.* **17** 29–38
[5] Dmitriev A I, Smolin A Yu, Psakhie S G, Osterle W, Kloss H and Popov V L 2008 *Phys. Mesomech.* **11** 73–84
[6] Eremin M, Kulkov A, Smolin I and Mikushina V 2019 *Frattura Integr. Strutt.* **13** (50) 38–45
[7] Bogomolov G N, Glazyrin V P and Orlov M Y 2016 *MATEC Web Conf.* **72** 01013
[8] Dong X, Shin C Y *J. Am. Ceram. Soc.* 2016 **99** (3) 1006–1014
[9] Schmauder S and Schäfer I 2016 *Multiscale Materials Modeling. Approaches to Full Multiscaling* (Berlin: De Gruyter) p 346
[10] Mikushina V A, Smolin I Yu 2018 *AIP Conf. Proc.* **2053** 030041
[11] Zhang C, Yang S *Materials* 2019 **12** (5) 727
[12] Smolin A Yu, Smolin I Yu and Smolina I Yu 2016 *Proc.Struc Integrity* **2** 2742–2749
[13] Balokhonov R R, Romanova V A 2009 *Int. J. Plast.* **25** 2025–2044
[14] Balokhonov R, Zinoviev A, Romanova V and Zinovieva O 2016 *Meccanica* **51** 415–428